Enhancement of the electrochemical activity of a commercial graphite felt for vanadium redox flow battery (VRFB), by chemical treatment with acidic solution of K2Cr2O7

Ali Hassan, Théodore Tzedakis

Enhancement of the electrochemical activity of a commercial graphite felt for vanadium redox flow battery (VRFB), by chemical treatment with acidic solution of $K_2Cr_2O_7$

Ali Hassan, Theodore Tzedakis*

Laboratoire de Génie Chimique, UMR CNRS 5503, Université de Toulouse-III Paul Sabatier, 118 Route de Narbonne, 31062 Toulouse, France

ARTICLE INFO

Keywords:
Vanadium redox flow battery
Chemical activation
Electroactivity enhancement
Carbon–oxygen catalytic sites
Graphite felt wettability
Charge–discharge electrolysis

ABSTRACT

The novel thermal-chemical activation method is proposed to prepare the graphite felt with highly functionalized surface and enhanced active surface area, to be used as the positive half-cell electrode for the vanadium redox flow batteries (VRFBs). The prescribed treatment consists of boiling the felt within $K_2Cr_2O_7$ solution in 5 M H_2SO_4, at different temperatures and time durations. It is time efficient, effective and durable. The cyclic voltammetry analysis enable to optimize the operating conditions i.e. boiling at 140 °C for 2 h. The activation treatment creates different surface oxygen functional groups, as characterized by FTIR, that act as catalytic sites toward the positive half-cell redox couple reaction ($VO^{2+} \rightleftharpoons VO_2^+$). Moreover, the improvement of various other properties of the graphite felt, resulted due to activation are also quantified, such as the surface roughness of fibers, the wettability toward electrolyte, the adsorption affinity against the vanadium and the surface energy of the graphite felt. The improved reversibility of VO^{2+}/VO_2^+ redox couple reaction against graphite felt is also evaluated and confirmed by the increase of intrinsic heterogeneous electronic transfer constant by 2.2 and 5.5 folds for the oxidation and reduction reactions, respectively. The performance evaluation of electrode at stack level by charge-discharge cycles, shows the improvement of the voltage efficiency and faradaic yield, as well as, the consistency of the performance over three cycles (~16 h).

1. Introduction

The power from the renewable energy recourses is acquiring a lot of attention due to huge pressing concerns about environmental issues and exhausting conventional power sources. Intermittent nature of the renewable energy induce limits on the practical and commercial viability of these resources [1,2]. A possibility to overcome limitations is the association of renewable energy sources to systems, named redox flow batteries, able to store important quantities of electroactive materials and consequently important quantities of energy [3]. For instance, vanadium redox flow batteries are successfully commercialized with significant energy density of 20–40 Wh/kg. Lithium ion redox flow batteries also offer 80–180 Wh/kg energy density, yet not commercially available. In recent times, various redox flow batteries have been investigated due to their large capacities, relatively economical costs, long life cycles and flexible operations i.e. Fe/Cr [4]; Sodium polysulfide/Br_2 [5]; V/Br_2 [6] and all vanadium redox flow batteries (VRFBs) [7]. The VRFBs was initially proposed by Skyllas Kazacos [8,9] and appears to be a promising and viable option due to the employment of the same metal ions in both electrolytic compartments, long electrolyte stability and minimized self discharge phenomena [3,10–13]. The positive and negative half cell reactions are described by the Eqs. (1) and (2) respectively. The theoretical overall cell voltage (ΔE^*) is 1.26 V.

$$\text{Positive half} - \text{cell reaction: } VO_2^+ + 2H^+ + e^- \rightleftharpoons VO^{2+} + H_2O \quad E^\circ(VO^{2+}/VO_2^+) = 1.00 \text{ V vs SHE;} \tag{1}$$

$$\text{Negative half} - \text{cell reaction: } V^{3+} + e^- \rightleftharpoons V^{2+} \quad E^\circ(V^{+2}/V^{+3}) = -0.26 \text{ V vs SHE;} \tag{2}$$

The selection of the electrode's material of VRFBs is critical in overall battery design, as it could exhibit high activation overpotentials for both redox couples. Besides, it should have high active surface area, low cost and good resistivity against acids [14]. Various carbon based materials were investigated like graphene oxide, graphite fibers, carbon paper, glassy carbon, graphite felt, carbon felt, multiwalled carbon

* Corresponding author.
E-mail address: tzedakis@chimie.ups-tlse.fr (T. Tzedakis).

https://doi.org/10.1016/j.est.2019.100967

nanotubes, etc. by different research groups [9,15 17], but most often they exhibit low electrocatalytic activity and poor kinetic reversibility for the vanadium redox couples. A lot of efforts have been done so far to improve the electrochemical performance of a carbon based electrodes, such as chemical or thermal treatment, electrochemical oxidation, doping of the chosen electrode by various metal/metal oxides i.e.: Pt, Pd, Au, Ir, Mn, Cu, Bi, Zr, etc [16,18,19 26,27 30].

The poly acrylonitrile (PAN) based graphite felt (GF) is widely used as electrode material in the vanadium redox flow batteries, due to highly resistive surface against acidic conditions, having low price and large specific surface area [23,31 33]. However, its electroactivity against the vanadium redox system appears to be poor and limit its applicability [17].

In literature, several treatments methods are intended to improve the vanadium reversibility against GF, most often as positive half cell electrode. Chemical activation of GF by Fenton reagents, resulted the improvements of around 5 10% in charge, voltage and energy effi ciencies [34]. GF decorated by carbon nanoparticles, introduced the improvement of 0.5 W/cm^2 [35]. Faradaic yield of 97% was observed at the current density of 500 A/m^2 by the microwave treated GF [36].

The present study focuses on the use of coupled thermal and che mical treatment, expecting to modify the surface of the GF to be used as positive half cell electrode in VRFBs. The study also quantifies the en hancement of the electrode activity in terms of the kinetic constant and the number of the created adsorption sites. A strong oxidizing agent i.e. potassium dichromate $K_2Cr_2O_7$ in sulfuric acid solution, is used to modify the electrode surface functionalities.

2. Experimental

2.1. Materials and chemicals

Poly acrylonitrile (PAN) based graphite felt (GF) of 3 mm thickness and platinum wire (0.125 mm, 99.95%) is provided by Goodfellow Cambridge Ltd. France. $VOSO_4{\cdot}5H_2O$ and $K_2Cr_2O_7$ are purchased from VWR international, France. The Nafion membrane (N 424) is provided by the Ion power Inc. USA. The sulfuric acid (95 97%) is purchased from the Sigma Aldrich Co. France.

2.2. Electrode activation

As received GF is thoroughly cleansed with distilled water in soni cator for 30 min. Then it is dried in the oven for 15 h at 50 °C and used as reference material for further use named as untreated GF. Untreated GF is heated at 400 °C for 5 h in the muffle furnace to burn away any greasy layer or impurities, adsorbed on its surface and then it is cut into six different pieces with dimension of 7 cm × 7 cm each. These pieces are treated as: the GF is boiled in a solution of $K_2Cr_2O_7$ (40 g/L) in 5 M H_2SO_4, at different temperatures ($100 < T_{(°C)} < 160$) and for various duration ($2 < t_{(h)} < 8$), under reflux conditions. In the following sec tions, the GF electrodes is named as: “oven temperature Cr duration of treatment in hours GF”; thus the “140 °C–Cr 5hrs GF” indicates that the piece of GF is boiled into the acidic solution of the dichromate at 140 °C for 5 h.

The expected general reaction while the activation of GF surface can be schematically written as;

$$Cr_2O_7^{2-} + k(-C-)_{groups} + k/2\ O_2 + 14\ H^+ \rightarrow 2Cr^{3+} + 7\ H_2O + k(-C-O-)_{groups} \quad (3)$$

After treatment, all the samples are thoroughly rinsed with deio nized water to remove all the residues of $Cr^{(III)\ or\ (VI)}$ and H_2SO_4, re mained on the electrode surface during the activation process followed by drying for 10 h at 50 °C in the oven for further use.

2.3. Electrode characterizations

The electrochemical activity of the GF is characterized by voltam metry; the experiments are performed in a classical three electrodes cell of 25 cm^3 capacity, containing the acidic solution of the vanadium. A piece of treated GF, having a certain surface delimited by a layer of glue, is used as working electrode; thin platinum wire (0.125 mm) in serted into the top side of the GF, act as current collector. The Saturated calomel electrode (SCE), immersed into a Luggin capillary and a pla tinum foil (~3 cm^2) are used as reference and counter electrodes, re spectively.

Two kinds of voltammetric curves are plotted:

i) *Cyclic voltammetry (CV) at the transient state*: The CV is performed using the Potentiostat workstation from OrigaLys ElectrochemSAS France, with operational parameters as; potential window: 0 1.6 V; scan rate: 10 mV/s; GF of 1 cm^2 geometrical area, immersed within unstirred solution of 0.05 M VO^{2+} + 2 M H_2SO_4.
ii) *Linear sweep voltammetry (LSV) at the steady state: $I = f(E)$* curves are plotted using the Potentiostat workstation from Metrohm Autolab pgstat 30, with operational parameters as; Scan rate: 1 mV/s, GF with 2.25 cm^2 geometrical area, immersed in a stirred solution at 350 RPM.

Two different solutions are used for linear sweep voltammetry (LSV):

- 0.5 M VO^{2+} is prepared by commercial salt of $VOSO_4$ dissolved in 3 M H_2SO_4, aiming to study the oxidation of VO^{2+} to $VO_2{}^+$.
- $0.43 < VO_2{}^+{}_{(M)} < 0.46$ + 3 M H_2SO_4 solution was obtained after a preparative electrolysis of VO^{2+} 0.5 M in 3 M H_2SO_4, (Section 2.4) in order to investigate the reduction of $VO_2{}^+$ to VO^{2+}.

The morphology of the untreated and treated GF surfaces is char acterized by the scanning electron microscopy (SEM) on Phenom XL (Thermo Fisher Scientific, USA) at an acceleration voltage of 10 kV. The surface functionalities are analyzed by the Fourier transform infrared spectroscopy (FTIR) on Thermo Nicolet 6700 (Thermo Fisher Scientific, USA). The 2.6 mg of GF sample is grinded, and the resulting powder is mixed with 250 mg dried potassium bromide and compressed under 10 ton of pressure to form the disk of 13 mm diameter for the analysis. In addition to FTIR analysis, the surface functionalities are also analyzed by the linear sweep voltammetry.

The high magnification digital camera is used to evaluate the hy drophilicity of GF electrodes as well as their surface energy, expected to control the electrolyte accessibility.

2.4. Half cell evaluations

As the purpose of the present study is to investigate the performance enhancement of the graphite felt toward the $VO^{2+}/VO_2{}^+$ reactivity on the positive electrode, the half cell is preferred against the complete cell, in order to minimize any kind of ohmic drop from other parts of battery stack.

The charge discharge cycles are performed in a classical H shaped cell. A rectangular band of GF with 2.25 cm^2 geometrical surface area is used as positive electrode. The negative electrode is a platinum foil (~3 cm^2). The anolyte contains 0.5 M VO^{2+} in 3 M H_2SO_4, while 3 M H_2SO_4 solution constitutes the catholyte.

A saturated calomel electrode (SCE) immersed into a Luggin capil lary is introduced in the positive electrode compartment of the half cell and is used as reference electrode, to follow the potential of the working electrode. Two electrolytic compartments are separated by a nafion membrane, clamped between two gaskets to avoid leakages. The elec trolyte in the positive electrode compartment is continuously stirred with magnetic bar at 350 RPM. There is no mechanical stirring of the

solution in the compartment of the counter electrode, except the con vection created by the H_2, produced from the proton reduction during electrolysis. Galvanostatic electrolysis is performed for charge/dis charges cycles, starting by the oxidation of the VO^{2+} solution. The magnitude of the applied current is 0.15 A/2.25 cm^2 (i.e. 660 A/m^2) and the electrolysis is stopped immediately as the electrode potential reaches 1.65 V/SCE, to avoid the oxidation of water. For the reduction of the electrogenerated VO_2^+, the same magnitude of the current (−0.15 A) is applied, and as the electrode potential reaches 0.75 V/ SCE, this current is immediately decreased to −0.1 A. The electrolysis is stopped when the electrode potential reaches 0.7 V/SCE to avoid any reduction of $V^{(IV)}$ to $V^{(III)}$. Periodically aliquots are taken to monitor the concentration of the $V^{(IV)}/V^{(V)}$ by UV/Visible spectroscopy (UV/VIS LAMBDA 365 Spectropho tometer). The Faradic yield of the electrode is calculated by the Eq. (4)

$$\text{Faradic yield} = \frac{\text{Theoretical charge required for the achieved conversion}}{\text{Actual charge provided for the achieved conversion}} \times 100 \quad (4)$$

3. Results and the discussions

3.1. Cyclic voltammetry (CV) and optimization of treatment parameters

Cyclic voltammetry is performed to evaluate the electrocatalytic activity of the different samples of GF and to find the optimal operating conditions of the treatment, that provide the best reversibility of the redox system VO^{2+}/VO_2^+ against these treated electrodes.

To evaluate the effect of the treatment, various electrochemical parameters from the voltammograms are compared and discussed, such as the anodic (I_a) and the cathodic (I_c) peak currents, the difference between anodic and cathodic peak potentials ($\Delta E_{a/c} = E_a - E_c$), as well as the ratio of the anodic to cathodic peak currents (I_a/I_c).

Fig. 1 presents, comparatively, the obtained voltammograms of all the treated electrodes at different conditions of temperature and time. The curve of the untreated electrode is also indicated in all the four plots and every parameter is compared to the corresponding parameter of the untreated electrode.

Following general remarks concern all the cyclic voltammograms of the Fig. 1:

i) All the CV experiments are started with the solution of VO^{2+} in the anodic side. Curves exhibit one signal in the range of 1.1 1.3 V, attributed to one electron oxidation of the VO^{2+} to VO_2^+. There is not any well defined reduction peak observed on the untreated GF; the reverse cathodic curve contains two successive shoulders. Conversely, for all the treated electrodes, reduction curve exhibits a single and well resolute signal, attributed to the reduction $VO_2^+ \rightarrow VO^{2+}$.

For the untreated electrode, the anodic amount of charge appears to be the same (± 15%) as the cathodic amount of charge.

The cathodic peak obtained with the treated electrode is located at the same potential (0.5/0.6 V) like the first shoulder obtained with the untreated electrode, it represents the $VO_2^+ \rightarrow VO^{2+}$ reaction. The oxidation of the vanadium (IV), i.e. VO^{2+} leads to the vanadium (V) i.e. VO_2^+ of which a part is adsorbed on the graphite (this will confirmed in the next sections). This part increase if the graphite is activated by the treatment. Thus, when VO^{2+} is oxidized, a part remains adsorbed on the fibbers and the rest leaves the electrode and disperses into the so lution, because the low potential scan rate 10 mV/s.

The second observed shoulder, located in the potential range of 0.2 0.3 V, is attributed to the reduction of $V^{(IV)}$ to V^{3+}. A part of the $V^{(IV)}$ is produced by the reduction of the $V^{(V)}$, but the main reduced quantity of $V^{(IV)}$ arrives by diffusion from the solution during the reverse scan because of the low potential scan rate. Note that, this second shoulder at 0.2 V is also observed if the solution of VO^{2+} is directly submitted to the reduction on the untreated electrode. Besides, the treatment of the graphite felt appears to decreases its affinity against the reduction of the of VO^{2+}, certainly because the saturation of the fibber surface of the felt by the adsorption of the $V^{(V)}$.

ii) The curves of treated electrodes show higher anodic and cathodic peak currents as compared to the untreated electrode; a possible explanation could be the increase of the available surface area of the fibers, typically due to the enhancement of the roughness of the electrode.

iii) The anodic to cathodic peak current ratio (I_a/I_c) observed for all curves is always higher than 1 as compared in Fig. 2. Theoretically, the unity value of the ratio means that: a) all the anodic current is used for the $V^{(IV)} \rightarrow V^{(V)}$, b) all the electrogenerated $V^{(V)}$ is retained/ adsorbed/ at the fibers surface and c) all the electrogenerated $V^{(V)}$ is reduced back to $V^{(IV)}$. This correspond to the condition of the re versibility.

The I_a/I_c ratio higher than one indicates that the oxidation of the $V^{(IV)}$ leads to the $V^{(V)}$, a part of which remain adsorbed on the GF and the rest leaves the electrode and disperses into the solution by diffusion before reducing back, especially at chosen low potential scan rate (10 mV/s). The adsorption tendency increases with treatment; so, the ratio tends to approach 1 as the electrocatalytic activity of the electrode increases. To sum up, the decrease of the ratio from 1.7 to 1.2 as function of the treatment, clearly demonstrates the improvement of the affinity of the electrode toward vanadium, thus revealing the en hancement of the reversibility of the VO^{2+}/VO_2^+ couple on GF.

For one electron transfer reversible processes, the difference be tween anodic and cathodic peak potential ($\Delta E_{a/c} = E_a - E_c$) is theo retically equal to 59 mV [37]. Due to activation of GF, the observed $\Delta E_{a/c}$ decreases from 0.99 V to 0.61 V, revealing the improvement in the electroactivity of GF. In this study, measured peak potential difference ($\Delta E_{a/c}$) of all treated electrodes is more than 10 times higher in com parison with the $\Delta E_{a/c}$ of the theoretical one electron reversible process, thus translating that the redox system has a low rate of the electronic transfer, even after improvement by treatment (Figs. 1 and 2). This point is more elaborated in Section 3.2

In the following section, Fig. 1 is discussed more specifically and results are compared in Fig. 2. The Fig. 1a is showing the effect of temperature from 100 °C to 160 °C at constant duration of 2 h. The observed peak current ratios (I_a/I_c) and potential differences ($\Delta E_{a/c}$) are 1.42, 1.23, 1.33, and 0.69 V, 0.61 V, 0.70 V at the temperatures of 100 °C, 140 °C and 160 °C, respectively. These results show that the 2 h treatment at 140 °C appears to be most suitable, as it leads to the lowest current ratio (I_a/I_c = 1.23) and the lowest peaks potential difference ($\Delta E_{a/c}$ = 0.61 V), in comparison with 2.1 and 0.99 V for untreated GF, respectively (Fig. 2). It is important to note that for higher temperatures than 140 °C, the performance of the graphite felt seems to deteriorate. Possibly at higher temperature of activation, the surface oxygen groups could be oxidized to various products including CO, CO_2. Moreover, graphite felt can be also be exfoliated and subsequently dissolved in acidic solution at high temperature, thus providing graphene or gra phene oxide [38]. Very strong oxidation conditions can also rapture the overall fibrous structure of the graphite felt.

Fig. 1b shows the effect of treatment duration, from 2 to 8 h under isothermal conditions of 100 °C. The improvement of the electroactivity of the GF is observed until 5 h and then starts decreasing for longer durations. At 100 °C, the best performance is obtained at 5 h treatment by 100 °C Cr 5hrs GF (I_a/I_c = 1.4; $\Delta E_{a/c}$ = 0.66 V). Even though, this performance is slightly lower than 140 °C Cr 2hrs GF as shown in Fig. 2.

The effect of duration is also studied at 140 °C as shown in Fig. 1c and results suggested that the shorter treatment duration is more ef fective on both peak current magnitude ratios, as well as, on the peak

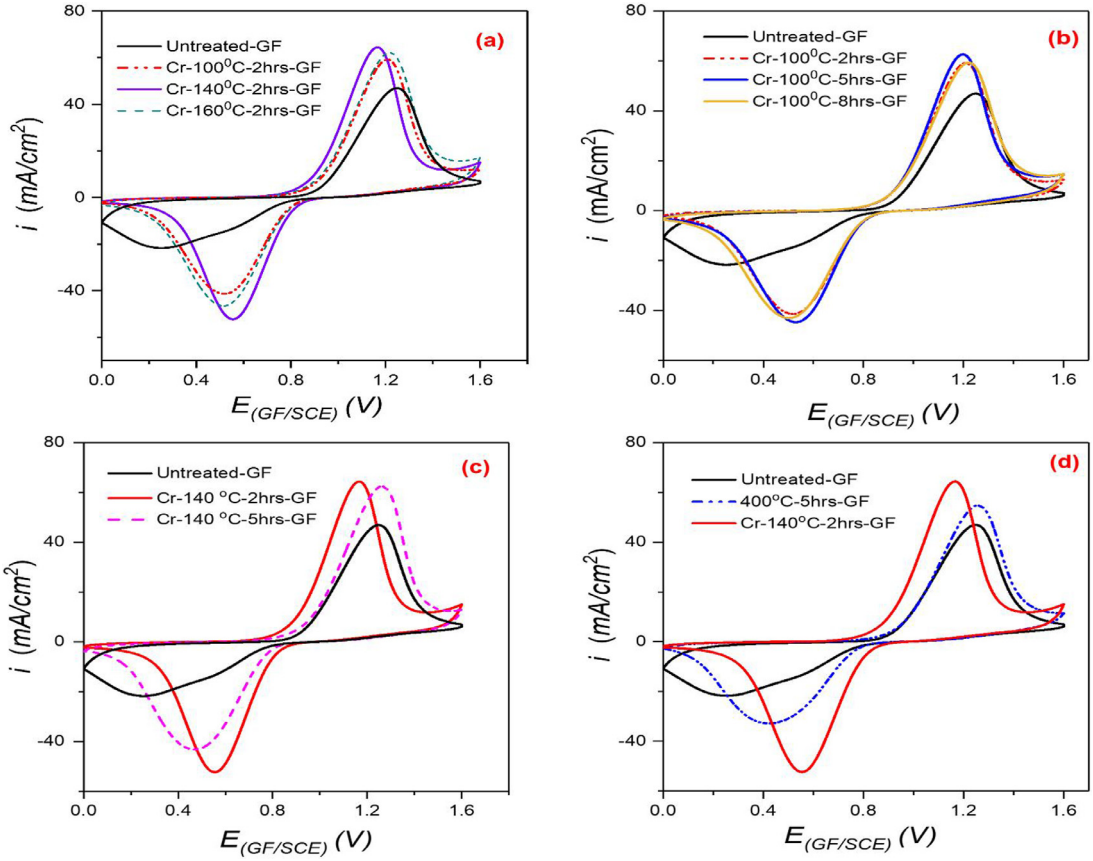

Fig. 1. Voltammograms of untreated and treated GF under unstirred conditions in 0.05 M VO^{2+} + 2 M H_2SO_4; r = 10 mV/s; S_{GF} = 1 cm²; CE = Pt mesh of ~3 cm². a) : Effect of temperature at 2 h; b) Effect of the duration at 100 °C; c) Effect of the duration at 140 °C; d) Effect of the thermal treatment.

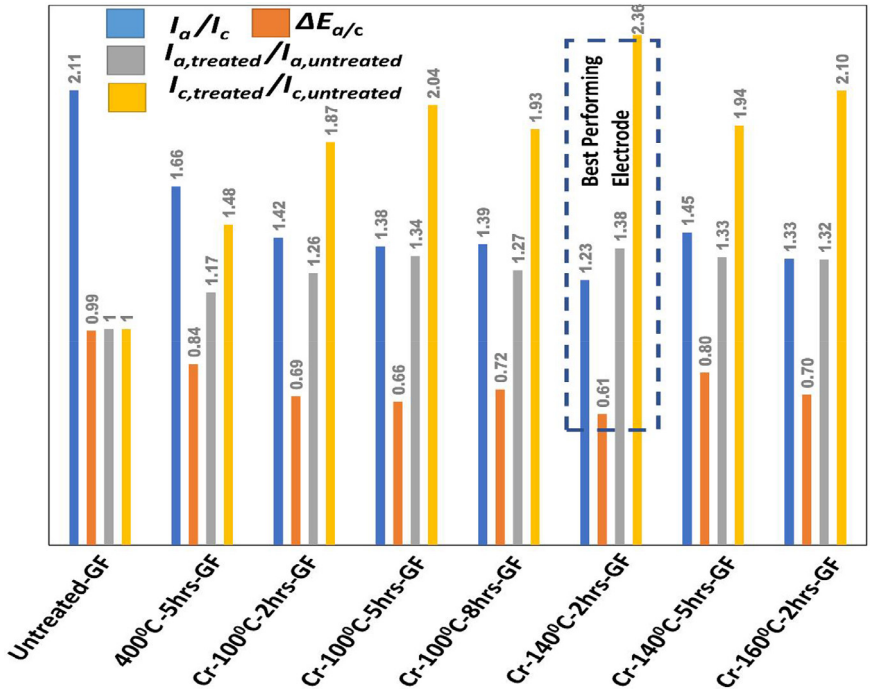

Fig. 2. Comparison of I_a/I_c, $I_{a,treated}/I_{a,untreated}$, $I_{c,treated}/I_{c,untreated}$ and $\Delta E_{a/c}$ between different treated graphite felt samples and untreated-GF (results extracted from Fig. 1).

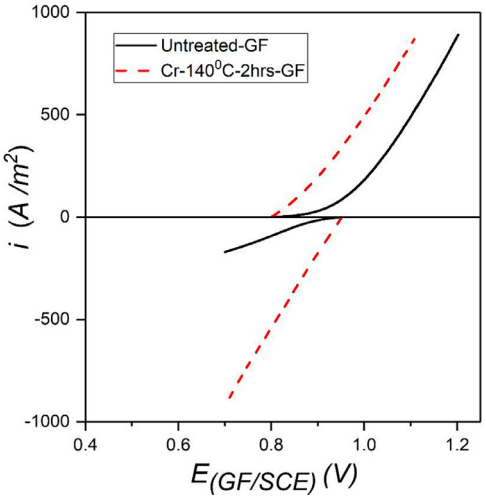

Fig. 3. Comparative current-potential curves obtained at the steady state, on Cr-140 °C-2hrs-GF and untreated-GF electrodes for vanadium redox system. S_{GF} = 2.25 cm²; r = 1 mV/s; CE = Pt ~3 cm; electrolyte: 3 M H_2SO_4; stirring: 350 RPM; Oxidation: 0.5 M of commercial VO^{2+}; Reduction: 0.43 M - 0.46 M solution of VO_2^+ obtained by electrolysis.

potential differences (Fig. 2).

In the activation process of GF, all the samples are heated in furnace at 400 °C for 5 h before the treatment with the acidic solution of $K_2Cr_2O_7$. During the manufacturing process of GF, various types of products could possibly adsorbed on the felt and in order to remove these products, the GF samples are annealed before activation process with dichromate [39 41]. The thermal treatment prior to chemical treatment, positively contributes in the GF activation process as shown in Fig. 1d. All the results of cyclic voltammetry are summarized in Fig. 2 for comparison. To conclude, the boiling of the electrode into a solution of $K_2Cr_2O_7$ + H_2SO_4 at 140 °C for 2 h under reflux conditions, provides the best results in the terms of the oxidation of $V^{(IV)}$ and the reduction of $V^{(V)}$. The proposed activation procedure is time efficient, economical and easy.

3.2. Linear sweep voltammetry (LSV)

In order to quantify the enhancement of the electrochemical activity of the graphite felt after treatment and to determine the corresponding kinetic parameters, linear sweep voltammetry is performed at the steady state for both, Cr 140 °C 2hrs GF and untreated GF. The examined potential range of the positive electrode of the battery corresponds to $0.7 < E_{\oplus\, in V/SCE} < 1.2$. Fig. 3 clearly indicates that the treatment by the dichromate has positive effect on the kinetics of both oxidation and reduction reactions.

The logarithmic analysis of the curves in electronic transfer limited region i.e. for $\eta \leq |0.1\ V|$, enables to determine the kinetic parameters i.e. the intrinsic heterogeneous electronic transfer constant $k^\circ_{an\ or\ cath.}$, α or β by Eqs. (5) and (6).

$$I = n\ F\ S\ k^\circ C_{bulk}\ \exp\frac{(+\alpha\ or\ -\beta)nF}{RT}(E_{I\neq o} - E_{I=o}) \quad (5)$$

$$\eta = -\frac{RT}{(+\alpha\ or\ -\beta)nF}\ln(nFSk^\circ C_{bulk}) + \frac{RT}{(+\alpha\ or\ -\beta)nF}\ln I = a + b\ log\ i \quad (6)$$

Where:

I, n, S, F and k° are respectively the current, the electrons exchanged number, the surface area, the faradic constant and the intrinsic heterogeneous electronic transfer constant;

α and β represent respectively the anodic and cathodic electronic transfer coefficients;

$E_{I\neq o} - E_{I=o}$ is the overvoltage η.

Table 1
Kinetic parameters of the VO_2^+/VO^{2+} system on treated and untreated GF electrodes.

Electrode used	Reaction involved	α	β	k° μm/s (this study)	k° μm/s [42]
Untreated	$VO^{2+} \rightarrow VO_2^+$	0.1	–	1.7	0.18
Treated		0.15	–	3.8	0.245
Untreated	$VO_2^+ \rightarrow VO^{2+}$	–	0.1	0.92	0.10
Treated		–	0.12	5.06	0.15

The Table 1 gives the results of the logarithmic analysis of the I/E curve of Fig. 3.

The treatment increases the intrinsic heterogeneous electronic transfer constant k° of $VO^{2+} \rightleftharpoons VO_2^+$, 2.2 folds for the oxidation reaction and 5.5 folds for the reduction reaction. Two facts could explain this behavior: i) the increase of the interfacial concentration of the C oxygen groups and hence the improvement of the vanadium affinity toward the GF; ii) the creation of more than one type of carbon oxygen groups on the GF surface, which can also contribute to the increases in the rate of vanadium oxidation and reduction reactions.

3.3. Surface characterization

The effect of the treatment on the roughness of the GF is examined by the scanning electron microscopy (SEM). Fig. 4 shows the images of the untreated GF (a, b, c), 400 °C 5hrs GF (d, e, f) and Cr 140 °C 2hrs GF (g, h, i), at different magnifications. The untreated GF (a, b, c) and 400 °C 5 h GF (d, e, f) have relatively smooth surfaces. It indicates that the treatment at 400 °C neither affect the overall fibrous structure of the felt significantly nor its surface roughness. The treatment, in presence of the dichromate, creates more roughness on the fibers and enhances their specific surface area available for vanadium adsorption, as shown in Fig. 4g, h, i. The overall fibrous structure of the GF is intacted after the activation procedure as there could not be seen any fragments of fibers.

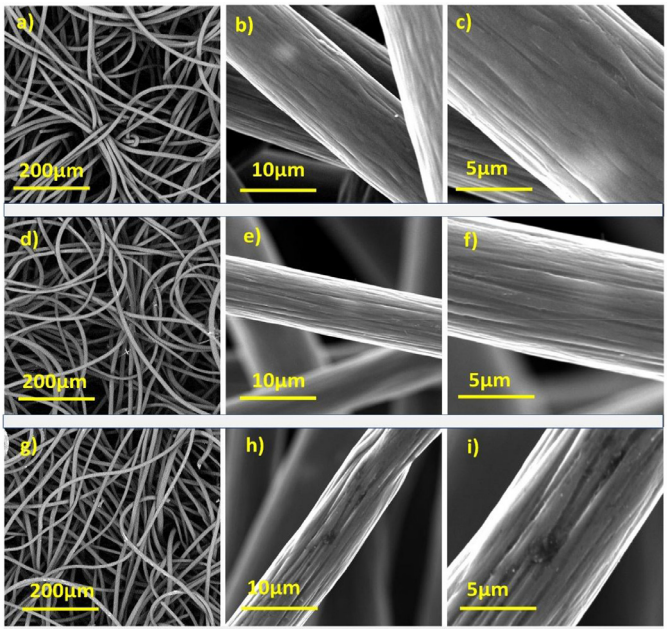

Fig. 4. Various magnification images obtained by scanning electron microscopy (SEM) for different graphite felt samples, at acceleration voltage of 10 kV. Untreated-GF(a, b, c); 400 °C-5h-GF (d, e, f); Cr-140 °C-2hrs-GF: (g, h, i).

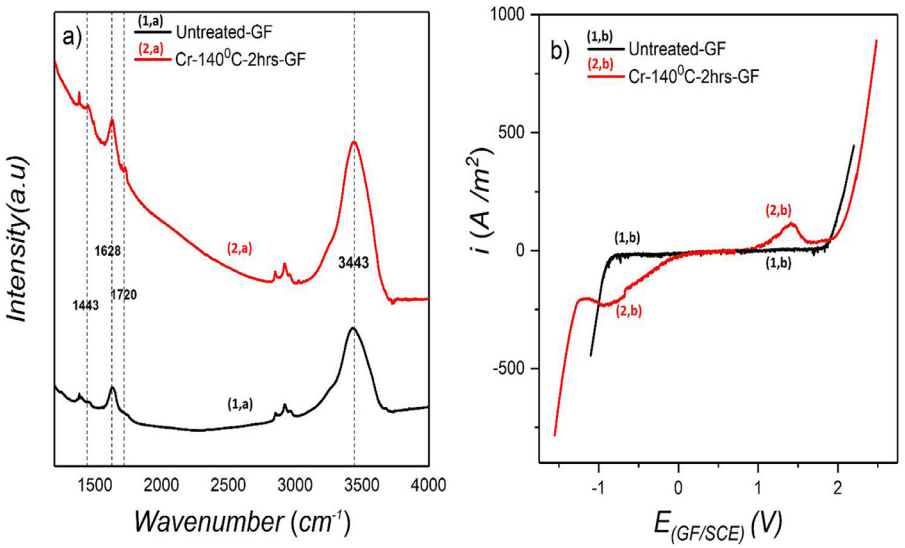

Fig. 5. Characterization of the GF by Fourier-transform infrared spectroscopy (FTIR) (a), and by linear sweep voltammetry (LSV) (b). For LSV/b: S_{GF} = 2.25 cm^2; r = 1 mV/s; CE = Pt ~3 cm^2. Stirred solution of 3 M H_2SO_4 by magnetic bar at 350 RPM.

Fourier transform infrared spectroscopy (FTIR) is used to char acterize the presence of oxygen groups and their chemical nature on the felt. There are different peaks evolved after treatment as shown in Fig. 5a. The peaks at 3440 cm^{-1} and 1450 cm^{-1} represent the stretching vibrations of hydroxyl group (−OH). The intensity of the peaks at 3440 cm^{-1} and 1450 cm^{-1}, enhanced as compared to the untreated sample, indicates the increment of hydroxyl groups [36]. Besides, the magnitude of the peak at 1628 cm^{-1}, assigned to the hy droxyl group in enol (−C═C−OH) [34], seems to increase after treat ment by the dichromate. Another important difference between the compared curves, is the new peak appearing at 1728 cm^{-1} and at tributed to the stretching vibration of the carbonyl group (C═O) [43,44]. To summarize, comparison of the FTIR spectra demonstrates that the treatment by dichromate is responsible for the formation of oxygenated groups on the surface of the GF; however, this method does not enable to quantify the concentration of these groups.

Linear sweep voltammetry is also used to confirm the existence of the oxygen groups on the felt. Fig. 5b shows the voltammogram ob tained at the steady state with the treated and untreated GF in the electrolyte of 3 M H_2SO_4 solution. The LSV curve of the untreated GF only shows the oxygen and hydrogen evolution at 1.88 V and −0.88 V, respectively. Between this potential window, there is not any other oxidation nor reduction observed. Conversely, the voltammogram ob tained with the Cr 140 °C 2hrs GF under the same set of conditions shows, in addition to the oxygen and hydrogen evolution, one anodic peak at 1.5 V and one cathodic peak at −0.6 V. These peaks are at tributed to the oxidation and reduction of the carbon oxygen groups present on the surface of treated felt, respectively. At 1.5 V, lower carbon oxidation state groups like hydroxyl group (C−OH) oxidize to higher oxides such as carboxylic and carbonyl groups (COOH, C═O) and vice versa for reduction side at −0.5 V [45].

3.4. Determination of adsorption sites

The activation overpotentials of the VO^{2+}/VO_2^+ redox couple re action on the GF decrease as the adsorption tendency of vanadium species enhanced on GF [29]. To check the adsorption capacity of the GF toward vanadium compounds and to validate the efficiency of the treatment, the number of the surface sites available to the adsorption of the vanadium is quantified.

The precisely cut samples of each untreated GF, 400 °C 5hrs GF and Cr 140 °C 2hrs GF are dipped in the 0.5 M $VOSO_4$ + 3 M H_2SO_4 solu tion for 5 min. After, the samples are taken out and thoroughly rinsed with 3 M H_2SO_4. Cyclic voltammetric curves are plotted in the unstirred

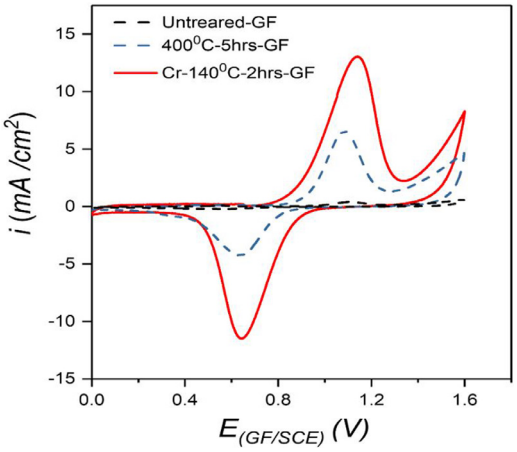

Fig. 6. Cyclic Voltammetric curves obtained using untreated-GF, 400 °C-5h-GF and Cr-140 °C-2h-GF, previously immersed in the solution of VO^{2+} 0.5 M + 3 M H_2SO_4 for 5 min, and then rinsed with 3 M H_2SO_4. Electrolyte: 3 M H_2SO_4 unstirred solution; at 10 mV/s potential scan rate; S_{GF} = 1 cm^2; CE = Pt ~3 cm^2. First scan in the anodic direction.

solution of 3 M H_2SO_4 and the results are presented in Fig. 6. The un treated GF exhibits low magnitude signals of current i.e. $I_{(an.\ or\ cath.\ Peaks)} < 1$ mA/cm^2, showing the quasi absence of any adsorption of the $VOSO_4$ at its surface.

The curve obtained by using 400 °C 5hrs GF exhibits:

an anodic peak of 6 mA/cm^2 between the potential range of 0.8 1.3 V, attributed to the oxidation of the adsorbed $V^{(IV)}$ and,
a cathodic peak of 4.5 mA/cm^2 between the potential range of 0 0.6 V, attributed to the reduction of the electrogenerated $V^{(V)}$.

The 140 °C Cr 2hrs GF shows the anodic peak of 14 mA/cm^2 and the cathodic peak of 12 mA/cm^2, almost doubled than thermally treated GF, implying a higher adsorption sites and consequently a better ad sorption capability of the GF against the vanadium species.

The peaks of these voltammetric curves are used to determine the number of the adsorption sites on GF. This number is assumed to be equal to the number of molecules of vanadium converted and conse quently the number of oxygen groups on surface, as these molecules are supposed to be adsorbed firstly on the oxygen groups of the electrode surface and then react. The following calculative sequence is applied i.e. integration of the peaks → amount of charge → number of

Table 2
Determination of the number of adsorption sites/oxygenated carbon atoms of the GF, on the untreated-GF, 400 °C-5 h-GF and Cr-140 °C-2 h-GF.

	Untreated-GF	400 °C-5hrs-GF	Cr-140 °C-2hrs-GF
$Q_{(anodic\ peak)}$ (C)	0.01	0.14	0.32
a = number of molecules of VO^{2+} converted = number of adsorption sites = number of oxygen groups/cm^2 geometrical area of GF	5.3×10^{16}	87×10^{16}	200×10^{16}

molecules → number of sites → number of surface carbon oxygen groups.

The number "a" of the molecules of the vanadium ($VOSO_4$) ad sorbed and converted, are estimated by the formula = Net charge of the anodic peak (Q) × Avogadro number ($\mathcal{N}$)/(1_e-×$\mathcal{F}$) and the results are summarized in Table 2.

The GF used for these measurements is a parallelepiped sized as 1.5 cm × 1.5 cm × 0.5 cm = 2.53 cm^3.

For the treated GF, the results lead to 200 × 10^{16} molecules of vanadium adsorbed on the fibers of GF having a volume of 2.53 cm^3. As per assumption, the obtain number of molecules of vanadium corre sponds to the number of C—O groups present on the GF fibers surface.

To get a rough estimation of the C—O groups on the GF fibers sur face, we draw a parallel between the atoms of platinum presents on a smooth surface of a platinum plate, i.e. 10^{15} atoms/cm^2. Equivalent surface of the Cr 140 °C 2hrs GF = (200×10^{16} atoms/2.53 cm^3)/(10^{15} atoms/cm^2) = 790 cm^2/cm^3 in comparison with 21 cm^2/cm^3 for the untreated GF. This equivalent surface appears to be high, especially for the GF fibers which appears to not have internal porosity into the fibers (Fig. 4). However, it shows that the GF exhibits high specific area and this is very important for an optimized vanadium battery.

Table 3
Measured surface energies of untreated and treated GF; γ_{GF} = Total surface energy; γ_{GF}^{D} = Dispersive component of total surface energy; γ_{GF}^{P} = Polar component of total surface energy.

	γ_{GF}^{P} (mN/m)	γ_{GF}^{D} = (mN/m)	γ_{GF} (mN/m)
Untreated GF	0.9	23.7	24.6
Cr-140 °C-2hrs-GF	15.9	13.7	29.6

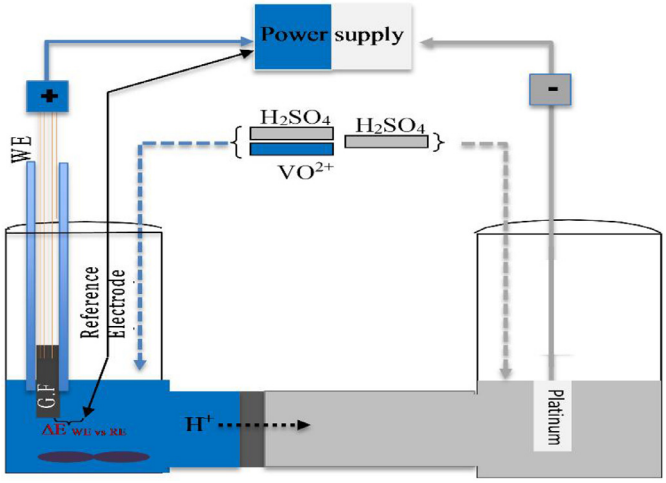

Fig. 8. Electrochemical reactor used for charge–discharge cycles of vanadium positive half-cell.

3.5. Wettability test

The commercial graphite felt appears to exhibit hydrophobic

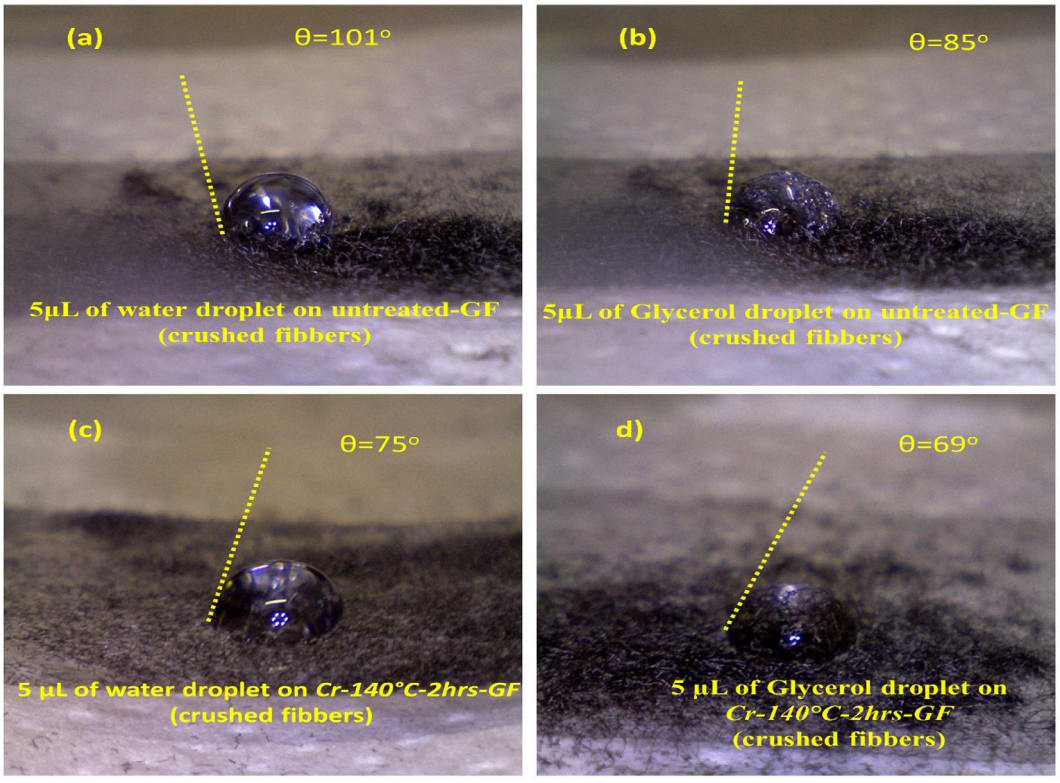

Fig. 7. Contact angle measurements on the grinded GF. Images on the top: water (a) and glycerol (b) droplets of 5 µL size, deposited on untreated GF.-Pictures on the bottom: water (c) and glycerol (d) droplets of 5 µL size, deposited on Cr-140 °C-2hrs-GF.

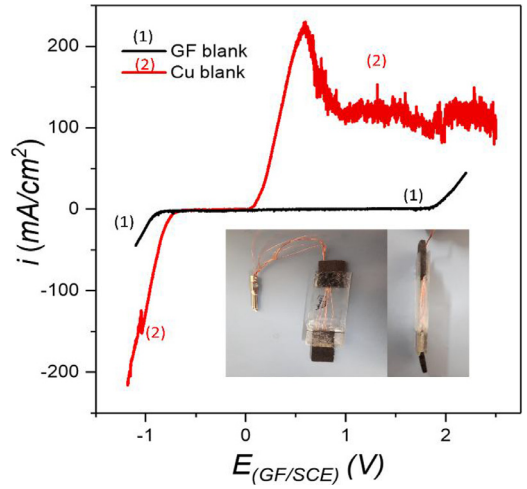

Fig. 9. Comparison between linear sweep voltammograms (LSV) obtained with the Electrode (A) and Electrode (B), used as working electrodes, in stirred 3 M H_2SO_4 aqueous solution as electrolyte. Stirring rate with a magnetic bar (350 RPM); r = 1 mV/s; RE: SCE immersed into a Luggin capillary; CE: Pt mesh. *Inset*: Specially designed positive half-cell electrode sandwiched between two glass plates with copper wires as current collector.

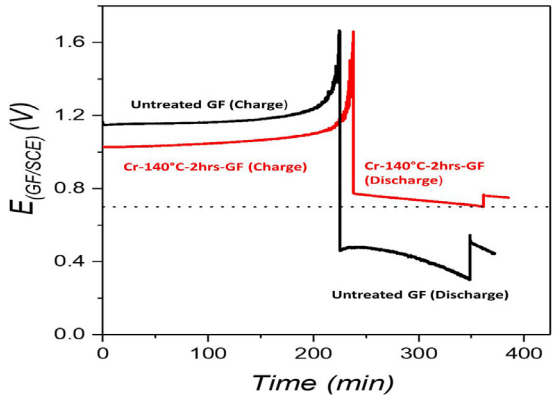

Fig. 10. Temporal evolutions of the GF potential during charge- discharge in a half-cell assembly, with untreated-GF and treated GF as 'Cr-140 °C-2hrs-GF' used as positive half-cell electrodes; S_{GF} = 2.25 cm^2; CE = Pt ~3 cm^2; positive half-cell electrolyte: 45 cm^3 0.5 M VO^{2+} in 3 M H_2SO_4 stirred at 350 RPM by a magnetic bar; electrolyte at the counter electrode compartment 3 M H_2SO_4.

behavior, though its hydrophobicity seems to be strongly dependent on its age and storage atmosphere. Another objective of the chemical thermal treatment of the GF by the dichromate is to improve its wett ability toward the vanadium sulfuric acid solution, expecting to enable all surface area of the electrode readily available for $VO^{2+} \rightleftharpoons VO_2^+$ re action. The hydrophilicity of the electrode, links with its surface energy, and is improved by the treatment (see supplementary data file).

The modification of the GF surface energy can be quantified by using the Owens Wendt one liquid method [46]. This technique enables the calculation of the surface energy of the electrode, by measuring the liquid contact angle of the two different liquid droplets of known polar and dispersive surface energy components on the solid surface as per Eqs. (7) and (8).

$$\gamma_{GF} = \gamma_{GF}^P + \gamma_{GF}^D \quad (7)$$

$$\gamma_L(1 + \cos\theta)/(2(\gamma_L^D)^{0.5}) = (\gamma_{GF}^P\ \gamma_L^P/\gamma_L^D)^{0.5} + (\gamma_{GF}^D)^{0.5} \quad (8)$$

Where:

γ_{GF}, γ_{GF}^P and γ_{GF}^P represent the total surface energy, dispersive and polar component of the surface energy of GF, respectively.

γ_L, γ_L^D and γ_L^P shows the total energy of the liquid, the dispersive and the polar component of the surface energy of the liquid, respectively. Moreover, θ shows the solid liquid contact angle.

Untreated and treated Graphite felts are crushed and spread over a hydrophobic flat tape. Then, 5 μL droplet of water (γ_L^D = 21.8 mN/m, γ_L^P = 51.0 mN/m) and glycerol (γ_L^D = 37.0 mN/m, γ_L^P = 26.4 mN/m) are carefully placed on the two flat surfaces having graphite felt powder. As shown in Fig. 7, the contact angle of the water and glycerol on the untreated GF surface is 101° and 85°, respectively and reduce to 75° and 69° after the activation of the GF. The $(\gamma_{GF}^P)^{0.5}$ and $(\gamma_{GF}^D)^{0.5}$ is obtained by the slop and intercept of the line, respectively by plotting the line between $\gamma_L(1 + \cos\theta))/(2(\gamma_L^D)^{0.5}$ and $(\gamma_L^P/\gamma_L^D)^{0.5}$.

The surface energy calculations are summarized in the Table 3. The activation of the GF induces 20.3% improvement in total surface energy of graphite felt. The polar surface energy component of GF increases from 0.9 mN/m to 15.9 mN/m, while the dispersive surface energy component decreased from 23.7 mN/m to 13.7 mN/m. It indicates that the chemical treatment replaces the weak electrostatic forces of the surface represented by dispersive component by stronger chemical bonds i.e. the polar component. As the GF surface have weak electro static forces because of defective carbon edges and delocalized π bonds [28,33] and these defective edges and delocalized bonds get oxidized by the chemical treatment. This observation is quite consistent with FTIR and LSV results that indicates the presence of oxygenated groups on the surface of treated graphite felt (Section 3.3)

3.6. Half cell evaluation

The performance of the treated graphite felt as the positive elec trode is evaluated by the charge discharge cycles in a H shaped classical cell (Fig. 8) by employing 0.5 M VO^{2+} + 3 M H_2SO_4 solution as posi tive half cell electrolyte and 3 M H_2SO_4 solution as negative half cell electrolyte. The special GF electrode assembly is prepared to avoid any kind of vibration because of strong stirring conditions as shown by inset of Fig. 9.

To prepare the assembly, a piece of the graphite felt (1.5 cm × 3 cm) is cut precisely; then a set of six copper wires that are acting as current collector, are inserted in this graphite felt, with;

- 1 cm length of each copper wire inside the felt, and
- 0.5 cm above from the surface area devoted for electrolysis.

A layer of an inert epoxy glue is introduced into the GF, to define precisely the electrochemically useful surface i.e. the bottom of the GF band. The glue also enables to avoid the contact of the copper wires i.e. the top of the GF band, with the solution. The structure is sandwiched between two glass plates with only 1.5 cm × 1.5 cm exposed surface area of the GF, available for the electrolyses. Before evaluating the

Table 4
Results of half-cell electrolysis using untreated-GF and Cr-140 °C-2hrs-GF electrode.

Electrode used	Conversion (%)		Faradic yield (%)		Average voltage (V)	
	Recharge	Discharge	Recharge	Discharge	Recharge	Discharge
Untreated-GF	87	48	95	73	1.19	0.42
Cr-140 °C-2hrs-GF	93	58	98	78	1.07	0.74

charge discharge performance of the electrode, it is important to ensure that the surface of GF involved in the reaction is precisely defined and there is not any reaction occurring in the other parts of the GF, nor in the epoxy glue used to define the perimeter of the working area. Hence, blank curves are plotted in 3 M H_2SO_4 electrolyte, as shown in Fig. 9, with two different working electrodes as follows;

i) Set of six copper wires with 1 cm length immersed into the electrolyte (Electrode A)
ii) The specially designed GF electrode assembly (Electrode B)

As shown in Fig. 9, the electrode (A) shows the huge anodic current starting from the 0 V that represents the oxidation of the copper wires. There is not any such signal in the curve of the electrode (B), except the evolution of oxygen and hydrogen is observed at ~1.8 V and ~ −0.9 V, respectively. It indicates that the solution is not diffusing upward till copper wires and epoxy glue is inert in the chosen operating conditions.

After evaluating the electrode assembly, the charge discharge cycles are performed to analyze the improvement occurred in the electrode due to treatment. The charging of positive half cell, i.e. the oxidation of the VO^{2+}, is achieved under constant anodic current of 0.15 A/2.25 cm^2. The electrolysis is stopped immediately as the electrode potential reach 1.65 V/SCE to avoid the oxidation of water. Fig. 10 shows the comparative evolution of working electrode potential for both charge and discharge cycles. During the oxidation phase, the potential stays at ~1.19 V and ~1.07 V for untreated and treated graphite felt, respectively. The activation of the electrode resulted in the decrease of the overvoltage of ~0.12 V during the whole oxidation ($0 < t_{(min)} < \sim 237$) and confirm the beneficial effect of the chemical treatment by the dichromate. The 94% and 87% conversion of $V^{(IV)}$ to $V^{(V)}$ is achieved for the treated and untreated GF, respectively. The 7% increment observed in the conversion for the treated electrode is because of the higher time required to reach 1.65 V due to the lowering of treated electrode potential. In addition to that, the charging faradic yield improves from 95% to 98%.

For the reduction of the electrogenerated $V^{(V)}$ to $V^{(IV)}$ a current of −0.15 A/cm^2 is applied and this current density is immediately reduced to 0.1 A/cm^2 as the potential of the treated GF reaches 0.75 V/SCE. The electrolysis is terminated when the electrode potential approaches 0.7 V/SCE to avoid any reduction of $V^{(IV)}$ to $V^{(III)}$. The treated graphite felt exhibits higher discharge potentials (~0.75 V) in comparison with untreated GF (0.4/ 0.3 V), showing the improvement of the reversibility of the graphite felt toward $V^{(V)}$ to $V^{(IV)}$ due to the activation. In addition to that, the treated electrode provides a certain stability of its potential during the reduction of $V^{(V)}$ to $V^{(IV)}$, comparatively to the untreated electrode in which no plateau is observed till 0.7 V. For the untreated GF, the discharge curve is observed around 0.4 V, below the limiting fixed value of the potential; this confirms that the raw graphite felt exhibits poor electroactivity toward the $V^{(V)} \rightarrow V^{(IV)}$ reaction.

For untreated and treated graphite felt, the same amount of charge is supplied during discharge, but vanadium $V^{(V)}$ to $V^{(IV)}$ conversion is different for both electrodes i.e. 48% and 58% for untreated and treated graphite felt, respectively. The possible reason of low discharge conversion in case of untreated electrode may be the overlapping of the secondary cathodic reaction of $V^{(IV)} \rightarrow V^{(III)}$ with the primary reaction i.e. $V^{(V)} \rightarrow V^{(IV)}$.

The three charge discharge cycles are performed with Cr 140 °C 2hrs GF successively. The performance of treated electrode remains stable over the three consecutive cycles (16 h), thus demonstrating that the enhanced electroactivity of the treated GF against the vanadium is durable. The performance of the untreated GF and Cr 140 °C 2hrs GF is compared in Table 4

4. Conclusion

The electrochemical activity of a commercial graphite felt, expected to be used as positive half cell electrode for vanadium redox flow batteries (VRFBs), is enhanced by thermal chemical treatment with $K_2Cr_2O_7$ solution in sulfuric acid. The graphite felt is boiled at different temperatures ($100 < T_{(°C)} < 160$) for different durations ($2 < t_{(h)} < 8$) in acidic dichromate solution, and afterward characterized by various physicochemical methods and techniques such as Fourier transform infrared spectroscopy, scanning electron microscopy, voltammetry, and high magnification digital camera. The treatment successfully modifies the surface chemistry and morphology of the GF by creating carbon oxygen functional groups and inducing roughness.

The results indicate that the best electrochemical performance is achieved by chemical activation at 140 °C for 2 h. The enhancement of the electrocatalytic properties of the graphite felt against the VO_2^+/VO^{2+}system is evidenced by voltammograms and preparative electrolysis results. In cyclic voltammograms, both $\Delta E_{a/c}$ and I_a/I_c ratio decrease respectively from 0.99 V to 0.61 V, and 2.11 1.23.

The enhancement of the electroactivity is also evidenced by the augmentation of the intrinsic heterogeneous electronic transfer constant k° by 2.2 folds for VO^{2+} oxidation and 5.5 folds for VO_2^+ reduction. Moreover, the carbon oxygen sites formed on the surface of the fibers, increases from 5.3×10^{16} to 200×10^{16} after activation.

The treated graphite felt appears to be efficient and durable as demonstrated by the three successive electrolysis. The prescribed thermochemical treatment of the GF offer several advantages for the vanadium batteries i.e. it is novel, operationally easy, effective as well as efficient and sustainable.

Financials

This work was supported by the Campus France and ANR (L'Agence nationale de la recherche, France).

Declaration of Competing Interest

The authors declare that there is no conflict of interest.

Acknowledgments

The authors would like to acknowledge Ms. Brigitte Dustou, Ms. Laure Latapie, Ms. Sandrine Desclaux, Ms. Alice Chourrier and Dr. Fabien Chauvet for the help and support they provided for the accomplishment of this work.

Supplementary materials

Supplementary material associated with this article can be found, in the online version, at doi:10.1016/j.est.2019.100967.

References

[1] N.R. Council, The National Academies Summit on America's Energy Future: Summary of a Meeting, The National Academies Press, Washington, DC, 2008, , https://doi.org/10.17226/12450.
[2] G. Kear, A.A. Shah, F.C. Walsh, Development of the all-vanadium redox flow battery for energy storage: a review of technological, financial and policy aspects, Int. J. Energy Res. 36 (2011) 1105–1120, https://doi.org/10.1002/er.1863.
[3] A.Z. Weber, M.M. Mench, J.P. Meyers, P.N. Ross, J.T. Gostick, Q. Liu, Redox flow batteries: a review, J. Appl. Electrochem. 41 (2011) 1137–1164, https://doi.org/10.1007/s10800-011-0348-2.
[4] Y.K. Zeng, T.S. Zhao, L. An, X.L. Zhou, L. Wei, A comparative study of all-vanadium and iron-chromium redox flow batteries for large-scale energy storage, J. Power Sources 300 (2015) 438–443, https://doi.org/10.1016/j.jpowsour.2015.09.100.
[5] H. Zhou, H. Zhang, P. Zhao, B. Yi, A comparative study of carbon felt and activated carbon based electrodes for sodium polysulfide/bromine redox flow battery, Electrochim. Acta. 51 (2006) 6304–6312, https://doi.org/10.1016/j.electacta.2006.03.106.

[6] H. Vafiadis, M. Skyllas-Kazacos, Evaluation of membranes for the novel vanadium bromine redox flow cell, J. Memb. Sci. 279 (2006) 394–402, https://doi.org/10.1016/j.memsci.2005.12.028.

[7] D.J. Park, K.S. Jeon, C.H. Ryu, G.J. Hwang, Performance of the all-vanadium redox flow battery stack, J. Ind. Eng. Chem. 45 (2017) 387–390, https://doi.org/10. 1016/j.jiec.2016.10.007.

[8] M. Rychcik, M. Skyllas-Kazacos, Evaluation of electrode materials for vanadium redox cell, J. Power Sources 19 (1987) 45–54, https://doi.org/10.1016/0378-7753(87)80006-X.

[9] B. Sun, M. Skyllas-Kazakos, Chemical modification and electrochemical behaviour of graphite fibre in acidic vanadium solution, Electrochim. Acta. 36 (1991) 513–517, https://doi.org/10.1016/0013-4686(91)85135-T.

[10] L. Cao, A. Kronander, A. Tang, D.W. Wang, M. Skyllas-Kazacos, Membrane permeability rates of vanadium ions and their effects on temperature variation in vanadium redox batteries, Energies (2016) 9, https://doi.org/10.3390/en9121058.

[11] C. Choi, S. Kim, R. Kim, Y. Choi, S. Kim, H. Young Jung, J.H. Yang, H.T. Kim, A review of vanadium electrolytes for vanadium redox flow batteries, Renew. Sustain. Energy Rev. 69 (2017) 263–274, https://doi.org/10.1016/j.rser.2016.11.188.

[12] M. Skyllas-Kazacos, L. Cao, M. Kazacos, N. Kausar, A. Mousa, Vanadium electrolyte studies for the vanadium redox battery—a review, Chem. Sus. Chem. 9 (2016) 1521–1543, https://doi.org/10.1002/cssc.201600102.

[13] L. Joerissen, J. Garche, C. Fabjan, G. Tomazic, Possible use of vanadium redox-flow batteries for energy storage in small grids and stand-alone photovoltaic systems, J. Power Sources. 127 (2004) 98–104, https://doi.org/10.1016/j.jpowsour.2003.09.066.

[14] K.J. Kim, M.-S. Park, Y.-J. Kim, J.H. Kim, S.X. Dou, M. Skyllas-Kazacos, A technology review of electrodes and reaction mechanisms in vanadium redox flow batteries, J. Mater. Chem. A. 3 (2015) 16913–16933, https://doi.org/10.1039/C5TA02613J.

[15] A. Di Blasi, O. Di Blasi, N. Briguglio, A.S. Aricò, D. Sebastián, M.J. Lázaro, G. Monforte, V. Antonucci, Investigation of several graphite-based electrodes for vanadium redox flow cell, J. Power Sources 227 (2013) 15–23, https://doi.org/10.1016/j.jpowsour.2012.10.098.

[16] C. Flox, J. Rubio-Garcia, R. Nafria, R. Zamani, M. Skoumal, T. Andreu, J. Arbiol, A. Cabot, J.R. Morante, Active nano-CuPt3 electrocatalyst supported on graphene for enhancing reactions at the cathode in all-vanadium redox flow batteries, Carbon N.Y. 50 (2012) 2372–2374, https://doi.org/10.1016/j.carbon.2012.01.060.

[17] A. Bourke, M.A. Miller, R.P. Lynch, X. Gao, J. Landon, J.S. Wainright, R.F. Savinell, D.N. Buckley, Electrode kinetics of vanadium flow batteries: contrasting responses of V^{II}-V^{III} and V^{IV}-V^{V} to electrochemical pretreatment of carbon, J. Electrochem. Soc. 163 (2016) A5097–A5105, https://doi.org/10.1149/2.0131601jes.

[18] W.H. Wang, X.D. Wang, Investigation of ir-modified carbon felt as the positive electrode of an all-vanadium redox flow battery, Electrochim. Acta. 52 (2007) 6755–6762, https://doi.org/10.1016/j.electacta.2007.04.121.

[19] K.J. Kim, M.-S. Park, J.-H. Kim, U. Hwang, N.J. Lee, G. Jeong, Y.-J. Kim, Novel catalytic effects of Mn_3O_4 for all vanadium redox flow batteries, Chem. Commun. 48 (2012) 5455, https://doi.org/10.1039/c2cc31433a.

[20] H. Zhou, Y. Shen, J. Xi, X. Qiu, L. Chen, ZrO_2-Nanoparticle-modified graphite felt: bifunctional effects on vanadium flow batteries, ACS Appl. Mater. Interfaces. 8 (2016) 15369–15378, https://doi.org/10.1021/acsami.6b03761.

[21] B. Li, M. Gu, Z. Nie, Y. Shao, Q. Luo, X. Wei, X. Li, J. Xiao, C. Wang, V. Sprenkle, W. Wang, Bismuth nanoparticle decorating graphite felt as a high-performance electrode for an all-vanadium redox flow battery, Nano Lett 13 (2013) 1330–1335, https://doi.org/10.1021/nl400223v.

[22] L. Wei, T.S. Zhao, L. Zeng, X.L. Zhou, Y.K. Zeng, Copper nanoparticle-deposited graphite felt electrodes for all vanadium redox flow batteries, Appl. Energy. 180 (2016) 386–391, https://doi.org/10.1016/j.apenergy.2016.07.134.

[23] W.W. Li, Y.Q. Chu, C.A. Ma, Highly hydroxylated graphite felts used as electrodes for a vanadium redox flow battery, Adv. Mater. Res. 936 (2014) 471–475, https://doi.org/10.4028/www.scientific.net/AMR.936.471.

[24] D.S. Kim, D.J. Chung, H.-I. Park, M.Z. Ansari, T. Song, H. Kim, Direct nitradated graphite felt as an electrode material for the vanadium redox flow battery, Bull. Korean Chem. Soc. 39 (2018) 281–286, https://doi.org/10.1002/bkcs.11380.

[25] Y.C. Chang, J.Y. Chen, D.M. Kabtamu, G.Y. Lin, N.Y. Hsu, Y.S. Chou, H.J. Wei, C.H. Wang, High efficiency of CO2-activated graphite felt as electrode for vanadium redox flow battery application, J. Power Sources 364 (2017) 1–8, https://doi.org/10.1016/j.jpowsour.2017.07.103.

[26] B. Sun, M. Skyllas-Kazacos, Modification of graphite electrode materials for vanadium redox flow battery application—I. Thermal treatment, Electrochim. Acta. 37 (1992) 1253–1260, https://doi.org/10.1016/0013-4686(92)85064-R.

[27] P. Mazúr, J. Mrlík, J. Beneš, J. Pocedič, J. Vrána, J. Dundálek, J. Kosek, Performance evaluation of thermally treated graphite felt electrodes for vanadium redox flow battery and their four-point single cell characterization, J. Power Sources 380 (2018) 105–114, https://doi.org/10.1016/j.jpowsour.2018.01.079.

[28] W. Zhang, J. Xi, Z. Li, H. Zhou, L. Liu, Z. Wu, X. Qiu, Electrochemical activation of graphite felt electrode for VO2+/VO2+ redox couple application, Electrochim. Acta. 89 (2013) 429–435, https://doi.org/10.1016/j.electacta.2012.11.072.

[29] Z. He, Y. Jiang, H. Zhou, G. Cheng, W. Meng, L. Wang, L. Dai, Graphite felt electrode modified by square wave potential pulse for vanadium redox flow battery, Int. J. Energy Res. 41 (2017) 439–447, https://doi.org/10.1002/er.3626.

[30] Y. Shao, X. Wang, M. Engelhard, C. Wang, S. Dai, J. Liu, Z. Yang, Y. Lin, Nitrogen-doped mesoporous carbon for energy storage in vanadium redox flow batteries, J. Power Sources 195 (2010) 4375–4379, https://doi.org/10.1016/j.jpowsour.2010.01.015.

[31] X. Gang Li, K. Long Huang, S. Qin Liu, N. Tan, L. Quan Chen, Characteristics of graphite felt electrode electrochemically oxidized for vanadium redox battery application, Trans. Nonferrous Met. Soc. China 17 (2007) 195–199, https://doi.org/10.1016/S1003-6326(07)60071-5 English Ed..

[32] D.M. Kabtamu, J.Y. Chen, Y.C. Chang, C.H. Wang, Water-activated graphite felt as a high-performance electrode for vanadium redox flow batteries, J. Power Sources 341 (2017) 270–279, https://doi.org/10.1016/j.jpowsour.2016.12.004.

[33] L.F. Castañeda, F.C. Walsh, J.L. Nava, C. Ponce de León, Graphite felt as a versatile electrode material: properties, reaction environment, performance and applications, Electrochim. Acta. 258 (2017) 1115–1139, https://doi.org/10.1016/j.electacta.2017.11.165.

[34] C. Gao, N. Wang, S. Peng, S. Liu, Y. Lei, X. Liang, S. Zeng, H. Zi, Influence of Fenton's reagent treatment on electrochemical properties of graphite felt for all vanadium redox flow battery, Electrochim. Acta. 88 (2013) 193–202, https://doi.org/10.1016/j.electacta.2012.10.021.

[35] L. Wei, T.S. Zhao, G. Zhao, L. An, L. Zeng, A high-performance carbon nanoparticle-decorated graphite felt electrode for vanadium redox flow batteries, Appl. Energy. 176 (2016) 74–79, https://doi.org/10.1016/j.apenergy.2016.05.048.

[36] X. Wu, H. Xu, P. Xu, Y. Shen, L. Lu, J. Shi, J. Fu, H. Zhao, Microwave-treated graphite felt as the positive electrode for all-vanadium redox flow battery, J. Power Sources 263 (2014) 104–109, https://doi.org/10.1016/j.jpowsour.2014.04.035.

[37] Z. González, C. Flox, C. Blanco, M. Granda, J.R. Morante, R. Menéndez, R. Santamaría, Outstanding electrochemical performance of a graphene-modified graphite felt for vanadium redox flow battery application, J. Power Sources 338 (2017) 155–162, https://doi.org/10.1016/j.jpowsour.2016.10.069.

[38] K. Parvez, Z.-S. Wu, R. Li, X. Liu, R. Graf, X. Feng, K. Müllen, Exfoliation of graphite into graphene in aqueous solutions of inorganic salts, J. Am. Chem. Soc. 136 (2014) 6083–6091, https://doi.org/10.1021/ja5017156.

[39] T.J. Rabbow, M. Trampert, P. Pokorny, P. Binder, A.H. Whitehead, Variability within a single type of polyacrylonitrile-based graphite felt after thermal treatment. Part II: chemical properties, Electrochim. Acta. 173 (2015) 24–30, https://doi.org/10.1016/j.electacta.2015.05.058.

[40] J. Langner, M. Bruns, D. Dixon, A. Nefedov, C. Wöll, F. Scheiba, H. Ehrenberg, C. Roth, J. Melke, Surface properties and graphitization of polyacrylonitrile based fiber electrodes affecting the negative half-cell reaction in vanadium redox flow batteries, J. Power Sources 321 (2016) 210–218, https://doi.org/10.1016/j.jpowsour.2016.04.128.

[41] T.J. Rabbow, M. Trampert, P. Pokorny, P. Binder, A.H. Whitehead, Variability within a single type of polyacrylonitrile-based graphite felt after thermal treatment. Part II: chemical properties, Electrochim. Acta. 173 (2015) 24–30, https://doi.org/10.1016/j.electacta.2015.05.058.

[42] E. Agar, C.R. Dennison, K.W. Knehr, E.C. Kumbur, Identi fi cation of performance limiting electrode using asymmetric cell con fi guration in vanadium redox fl ow batteries, 225 (2013) 89–94. doi:10.1016/j.jpowsour.2012.10.016.

[43] K.J. Kim, S.W. Lee, T. Yim, J.G. Kim, J.W. Choi, J.H. Kim, M.S. Park, Y.J. Kim, A new strategy for integrating abundant oxygen functional groups into carbon felt electrode for vanadium redox flow batteries, Sci. Rep. 4 (2014) 1–6, https://doi.org/10.1038/srep06906.

[44] L. Yue, W. Li, F. Sun, L. Zhao, L. Xing, Highly hydroxylated carbon fibres as electrode materials of all-vanadium redox flow battery, Carbon N.Y. 48 (2010) 3079–3090, https://doi.org/10.1016/j.carbon.2010.04.044.

[45] F. Mohammadi, P. Timbrell, S. Zhong, C. Padeste, M. Skyllas-Kazacos, Overcharge in the vanadium redox battery and changes in electrical resistivity and surface functionality of graphite-felt electrodes, J. Power Sources 52 (1994) 61–68, https://doi.org/10.1016/0378-7753(94)01938-X.

[46] D.K. Owens, R.C. Wendt, Estimation of the surface free energy of polymers, J. Appl. Polym. Sci. 13 (1969) 1741–1747, https://doi.org/10.1002/app.1969.070130815.